Available online at www.sciencedirect.com
ScienceDirect
Journal of Sound and Vibration 312 (2008) 1–18
JOURNAL OF SOUND AND VIBRATION
www.elsevier.com/locate/jsvi

Higher-frequency wavenumber shift and frequency shift in a cracked, vibrating beam

D.G. Kasper*, D.C. Swanson, K.M. Reichard

The Applied Research Laboratory, The Pennsylvania State University, State College, PA 16804, USA

Received 11 February 2005; received in revised form 19 February 2007; accepted 9 July 2007

Abstract

Explicit wavenumber shift and frequency shift expressions are derived for the resonances of a cracked, transversely vibrating beam. These explicit expressions apply to beams with both shallow and deeper cracks. The explicit expressions are approximate, however, and are therefore generally inaccurate for the fundamental beam mode, and for a crack located in a boundary near field. The explicit expressions indicate that wavenumber shift and frequency shift are approximately proportional to the potential energy in the uncracked beam at the (future) crack location. Experimental results are presented for a freely vibrating, free–free beam with a midspan, single-edge slot. Data was collected for bending about both the strong axis and the weak axis. The experimental wavenumber shift curves generally agree well with the theoretical wavenumber shift curves.

1. Introduction

Condition-based maintenance (CBM) is one of the major maintenance philosophies for machines and structures [1]. In a CBM architecture, maintenance decisions are based on both the current condition, or health, of a machine or structure, and the estimated future condition of the machine or structure. To obtain an estimate of machine or structure condition, however, measurable characteristics are needed that reflect the condition of the machine or structure [2, pp. 35–38, 241].

One characteristic of a machine or structure that can be used for condition monitoring is a resonance frequency, or resonance wavenumber. If a structure is cracked, for example, the structure generally experiences a decrease in overall stiffness [3–7]. Since the resonance frequencies and resonance wavenumbers of a structure depend on overall stiffness, the introduction and growth of a crack in a structure is reflected through changes in the resonance frequencies and resonance wavenumbers.

The focus of this work is the derivation of explicit wavenumber shift and frequency shift expressions for a cracked, lossless, transversely vibrating beam. These explicit wavenumber shift and frequency shift expressions are appropriate not only for beams with shallow cracks, but also for beams with deeper cracks. Given that the explicit frequency shift expressions available in the literature [6,8–12] generally apply only to beams with small

*Corresponding author. Current address: Sentient Corporation, 850 Energy Drive, Idaho Falls, ID 83401, USA. Tel.: +1 208 522 8560.
E-mail address: dkasper@sentientscience.com (D.G. Kasper).

0022-460X/$ - see front matter © 2007 Elsevier Ltd. All rights reserved.
doi:10.1016/j.jsv.2007.07.092

defects, the explicit expressions derived here can be used in conjunction with the explicit, small-crack expressions available in the literature to form a more complete picture of the failure process for a cracked structure. Note that the phrase "small crack" refers not to the physical size of the crack, but to the effective size of the crack [13,14]. In other words, a small crack is one that has a small effect on beam vibration, regardless of absolute crack length. Likewise, a deep crack is one that has a significant effect on beam vibration, regardless of absolute crack length.

The benefits of explicit expressions are that they help illuminate underlying damage physics, and they help clarify system dependencies. The tradeoff for these benefits, however, is that the expressions are limited in applicability. For example, the explicit expressions derived in this work are generally inaccurate for the fundamental beam mode. In addition, the explicit expressions derived here apply only for cracks located in the vibratory far field, the far field being all points on the beam at least one half-wavelength from a boundary. Another limitation of the explicit expressions derived in this work is that the expressions apply only to symmetric, uniform beams.

Explicit expressions are derived in this work using a series of approximations collectively called high-frequency approximations. The phrase "high frequency," however, is a little misleading because the approximations, and the resulting wavenumber shift and frequency shift expressions, are generally applicable to all but the lowest beam mode. The "high-frequency" terminology is used because the approximations tend to improve as frequency increases.

2. Background

A significant number of works have been published that relate to crack- or slot-induced changes in resonance frequencies. An overview of much of the work is available in several review papers [3–5,15–18]. Despite the substantial amount of work done in the field of crack-induced changes in resonance frequencies, only a small fraction of the work includes derivations of explicit solutions for frequency, frequency shift, or wavenumber shift. Since explicit wavenumber shift and frequency shift expressions are the focus of this work, the discussion given in this section includes only those authors who derive explicit frequency, frequency shift, or wavenumber shift expressions.

The number of published works regarding crack- or slot-induced changes in resonance frequencies is indicative of the number of different models available for damaged beams. One of the more common models used in the literature is the rotational spring model [8–10,19–23]. The rotational spring model involves modelling a cracked beam as two beam segments connected by a rotational spring. The rotational spring accounts for the additional flexibility introduced by the crack. The rotational spring model is the basis for the analysis given in this paper.

Morassi [8,24], Hasan [9], and Liang and Hu [6,10,11] all derive explicit solutions for frequency and frequency shift using the rotational spring model. Morassi gives an explicit frequency shift expression for a cracked beam vibrating in bending. Morassi derives this explicit frequency shift expression using a perturbation approach. Hasan uses an approach similar to Morassi's to derive an explicit frequency shift expression for a cracked beam on an elastic foundation. Hasan shows that frequency shift lacks an explicit dependence on the elastic foundation. Hasan's expression is therefore the same as Morassi's. Morassi's and Hasan's results are valid for symmetric beams terminated with rotational and translational springs. Morassi's and Hasan's results can also be applied to nonuniform beams. Liang and Hu derive an explicit frequency shift expression for a cracked beam vibrating in bending, but approach the problem using a Taylor series expansion.

Gudmundson derives an explicit expression for the resonance frequencies of a vibrating structure [12]. Gudmundson's expression is valid for a wide range of structures, including structures with defects and geometric modifications, and structures undergoing various types of vibration. Gudmundson uses an energy-based, perturbation approach to derive the explicit frequency expression. Gudmundson is the only author of those mentioned here who does not use the rotational spring model. Gudmundson's expression is also the only one of those mentioned here that can account for a loss of mass in addition to a loss of stiffness.

The expressions derived by Gudmundson, Morassi, Hasan, and Liang and Hu are all valid for any defect location, and are all valid for any mode in the Bernoulli–Euler region [19]. The main limitation of these explicit expressions, however, is that they are valid only for small defects.

Arzoumanian [25] derives explicit wavenumber shift expressions that are valid for a vibrating beam with a deeper crack. Arzoumanian obtains explicit solutions for wavenumber shift by applying high-frequency approximations to the characteristic equation obtained from the rotational spring model. Arzoumanian gives explicit wavenumber shift expressions for a beam with a sliding boundary crack, a beam with a clamped boundary crack, and a symmetric beam with a midspan crack. Arzoumanian also analyzes a beam with an arbitrarily located crack, but does not give an explicit wavenumber shift expression for the beam. The general procedure used to derive the explicit expressions in this work is similar to the general procedure used by Arzoumanian.

3. Wavenumber shift expressions

A cracked beam and the associated rotational spring model are shown in Fig. 1. The beam is assumed to be vibrating in flexure, and the uncracked beam is assumed to be uniform with a rectangular cross-section. The crack is assumed to be transverse and through-the-thickness. The other assumptions typically associated with the rotational spring model also apply [7,10,24,13, pp. 15–22].

The uncracked beam corresponding to Fig. 1 has a length L, a width h, a thickness t, and a cross-sectional area $A = ht$. Crack depth is denoted a, and the rotational spring in Fig. 1 has an equivalent compliance C_s.

The coordinate system for the beam is rectangular, with the origin at midspan. Axial position is ξ, axial crack location is ξ_s, and $-L/2 \leqslant \xi$, $\xi_s \leqslant L/2$. The quantity y is the coordinate in the thickness direction and z is the coordinate in the width direction.

Bernoulli–Euler beam theory is assumed to be valid everywhere in the model beam and beam segments. The transverse vibration of the beam is therefore described by the classical bending wave equation

$$\frac{\mathrm{d}^4 w(\xi)}{\mathrm{d}\xi^4} - k^4 w(\xi) = 0,$$

where time harmonic motion is assumed and $k^4 = \omega^2 \rho A/(EI)$. The quantity $w(\xi)$ is beam deflection, k is bending wavenumber, ω is radian frequency, ρ is material density, E is the modulus of elasticity, and I is the second moment of area.

Explicit solutions for wavenumber shift are obtained by applying high-frequency approximations to the characteristic equation associated with the rotational spring model. The characteristic equation is obtained by assuming a deflection for each sub-beam, and then plugging these two deflections into the appropriate continuity, compatibility, and boundary conditions. The deflections of the sub-beams are

$$w_1(\xi) = A_1 \sin\left[k\left(\frac{L}{2}+\xi\right)\right] + B_1 \cos\left[k\left(\frac{L}{2}+\xi\right)\right] + C_1 \sinh\left[k\left(\frac{L}{2}+\xi\right)\right] + D_1 \cosh\left[k\left(\frac{L}{2}+\xi\right)\right]$$

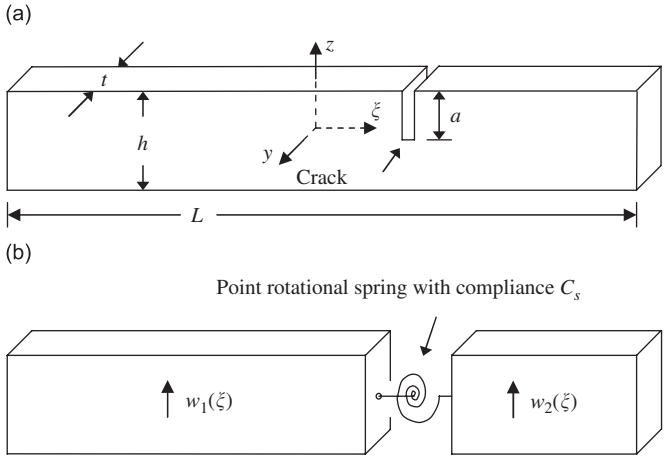

Fig. 1. A cracked beam (a) and the associated rotational spring model (b).

and

$$w_2(\xi) = A_2 \sin\left[k\left(\frac{L}{2} - \xi\right)\right] + B_2 \cos\left[k\left(\frac{L}{2} - \xi\right)\right] + C_2 \sinh\left[k\left(\frac{L}{2} - \xi\right)\right] + D_2 \cosh\left[k\left(\frac{L}{2} - \xi\right)\right].$$

The continuity and compatibility conditions at the crack location ξ_s are, after introducing prime notation,

$$w_1(\xi_s) - w_2(\xi_s) = 0,$$

$$w_1'(\xi_s) - w_2'(\xi_s) + \frac{4\gamma}{k_0} w_1''(\xi_s) = 0,$$

$$w_1''(\xi_s) - w_2''(\xi_s) = 0$$

and

$$w_1'''(\xi_s) - w_2'''(\xi_s) = 0.$$

The quantity γ is $EIk_0C_s/4$, where k_0 is the wavenumber for the undamaged beam and k is the corresponding wavenumber for the damaged beam.

The analysis given in this paper is limited to symmetric beams. The boundary conditions for the beam in Fig. 1 must therefore support this symmetry. Assume, then, that the beam is clamped at both ends. Although the wavenumber shift expressions are initially derived for a beam with clamped boundaries, the expressions are eventually generalized to symmetric beams with other boundary conditions.

The boundary conditions for the clamped–clamped beam are $w_1(-L/2) = 0$, $w_1'(-L/2) = 0$, $w_2(L/2) = 0$, and $w_2'(L/2) = 0$. The characteristic equation for a clamped–clamped beam with an arbitrarily located crack is

$$\begin{aligned}
&1 - \cos(kL)\cosh(kL) \\
&\quad + 4\gamma \frac{k}{k_0}\left\{\sin\left(k\frac{L}{2}\right)\cos\left(k\frac{L}{2}\right)\left[\cosh^2\left(k\frac{L}{2}\right) + \sinh^2(k\xi_s)\right]\right. \\
&\quad - \cos\left(k\frac{L}{2}\right)\sinh\left(k\frac{L}{2}\right)[\cos(k\xi_s)\cosh(k\xi_s) - \sin(k\xi_s)\sinh(k\xi_s)] \\
&\quad + \sin\left(k\frac{L}{2}\right)\cosh\left(k\frac{L}{2}\right)[\cos(k\xi_s)\cosh(k\xi_s) + \sin(k\xi_s)\sinh(k\xi_s)] \\
&\quad \left. - \sinh\left(k\frac{L}{2}\right)\cosh\left(k\frac{L}{2}\right)\left[\cos^2\left(k\frac{L}{2}\right) - \sin^2(k\xi_s)\right]\right\} = 0. \qquad (1)
\end{aligned}$$

The first two terms in Eq. (1) represent the characteristic equation for an uncracked, clamped–clamped beam.

Eq. (1) cannot be solved explicitly for wavenumber or wavenumber shift. An approximate, explicit solution for wavenumber shift, however, may be obtained for higher frequencies. Assume that the dimensionless wavenumber kL is large enough such that $\sinh(kL/2) \cong \cosh(kL/2) \cong e^{kL/2}/2$, and such that $2e^{-kL} \cong 0$ [26, p. 209, 27, p. 277]. Given that the dimensionless resonance wavenumbers for a clamped–clamped beam are approximately $kL = (m + 1/2)\pi$, where $m = 1, 2, 3, \ldots$ [28], the quantities $\sinh(kL/2)$ and $\cosh(kL/2)$ differ by 2% for the first mode ($m = 1$), by 0.08% for the second mode ($m = 2$), and by less then 0.004% for modes three and higher ($m \geqslant 3$). The difference between $\sinh(kL/2)$ and $\cosh(kL/2)$ decreases rapidly for increasing dimensionless wavenumber kL. The quantity $2e^{-kL}$ is 0.02 for the first mode, and less than 0.0008 for modes two and higher.

The approximation $\sinh(kL/2) \cong \cosh(kL/2)$ is a large-argument approximation. It is also a high-frequency approximation since the argument is proportional to wavenumber. Nevertheless, the approximation $\sinh(kL/2) \cong \cosh(kL/2)$ is generally valid for all but possibly the lowest beam mode. The physical implication of the approximation $\sinh(kL/2) \cong \cosh(kL/2)$ is that the boundary near field, represented by the

exponential decay terms in the solution to the bending wave equation, decays rapidly in space at higher frequencies, and is thus negligible with respect to overall beam deflection [29, pp. 125–126].[1] Overall beam deflection can therefore be adequately described by just the far-field deflection, which is dominated by the sinusoidal, or propagating wave, terms in the solution to the bending wave equation. As a result of neglecting the near-field contribution to overall beam deflection, the remaining equations in this section include sinusoidal functions only; the equations do not include hyperbolic functions. Note that although the near-field contribution to overall beam deflection is neglected, the boundaries still have an impact on frequency and spatial phase [30, p. 34].

In addition to assuming that beam deflection can be adequately characterized by the far-field contribution, assume that the crack is located in the far field. With this restriction on crack location, $\sinh(kL/2) \gg |\sinh(k\xi_s)|$ by more than a factor of 10 and $\sinh(kL/2) \gg \cosh(k\xi_s)$ by more than a factor of 10. Incorporating these inequalities into Eq. (1) as approximations, and applying the approximations of the previous paragraphs to Eq. (1) yields

$$\frac{\gamma k/k_0}{1+\gamma k/k_0}\sin(kL) - \cos(kL) = \frac{\gamma k/k_0}{1+\gamma k/k_0}\cos(2k\xi_s). \tag{2}$$

Eq. (2) is a better approximation of Eq. (1) for higher frequencies and for crack locations closer to midspan.

Eq. (2) may also be obtained from expressions given in the literature. Eq. (2) may be obtained from Arzoumanian [25, p. 53], Eq. (4.55), after shifting the coordinate system to midspan. Eq. (2) may be obtained from both Reznicek and Springer [22] and Narkis and Elmalah [23] by applying the procedure used to obtain Eq. (2) from Eq. (1). Both Arzoumanian and Reznicek give the characteristic equation for a free–free beam with an arbitrarily located crack. Narkis gives the characteristic equation for a cantilever beam with an arbitrarily located crack. Eq. (2) therefore applies not only to a clamped–clamped beam, but also to free–free and cantilever beams.

The quantity of interest is not absolute wavenumber, but is instead the absolute change in wavenumber. Mathematically, Δk is wavenumber shift and is given by $\Delta k = k_0 - k$. Eq. (2) may be rewritten in terms of wavenumber shift as

$$\sin(\Delta kL) - \mu\cos(\Delta kL) = \pm\mu\cos\left[2k_0\xi_s\left(1-\frac{\Delta k}{k_0}\right)\right], \tag{3}$$

where

$$\mu = \frac{\gamma(1-\Delta k/k_0)}{1+\gamma(1-\Delta k/k_0)}.$$

Eq. (3) is obtained by substituting $k_0 - \Delta k$ for k and by recognizing that, at higher frequencies, the characteristic equation for an uncracked, clamped–clamped beam is approximately $\cos(k_0L) = 0$. Note that the quantities k, k_0, Δk, γ, and μ all depend on the given mode m of interest.

The plus sign in Eq. (3) applies to the even-symmetric modes, meaning those modes having even-symmetric deflection about midspan. The minus sign in Eq. (3) applies to the odd-symmetric modes, meaning those modes having odd-symmetric deflection about midspan.

Eq. (3), like Eq. (2), applies to clamped–clamped, free–free, and cantilever beams. Eq. (3) also applies to simply supported beams. For example, Eq. (3) may be obtained from Narkis [7] by following the same steps used to obtain Eq. (3) from Eq. (1). Narkis gives the characteristic equation for a simply supported beam with

[1] Note the difference between the near-field components of beam deflection and the region of the beam defined as the near field. The near-field components of beam deflection are the exponential decay terms in the solution to the bending wave equation. These components contribute to beam deflection over the entire length of the beam, but are most significant within the region defined as the near field. The near field is defined here as the region of the beam within about one-half wavelength of either boundary [25]. Consequently, the far field consists of all points on the beam that are not in the near field. Wavelength may be estimated from wavenumber, for either the damaged or the undamaged beam, using the relation $\lambda = 2\pi/k$. Wavelength may also be estimated by doubling the distance between two adjacent, far-field deflection nodes. Note that the extent of the far field, and thus the region in which the wavenumber shift theory is valid, decreases with crack growth. This decrease, however, is generally small and inconsequential, especially for smaller cracks and higher frequencies.

an arbitrarily located crack. Generalizing even further, Eq. (3) applies to any symmetric beam with classical boundary conditions.

Note that Eq. (3), derived for symmetric beams only, is valid for a cantilever beam, an asymmetric beam. This apparent discrepancy is resolved by recognizing that, at higher frequencies, the far field deflection of a cantilever is nearly symmetric about midspan [26, p. 208, 28, pp. 110, 119–123, 29, pp. 121–130]; the asymmetry of the cantilever is due to the boundary near-field components, and is thus limited primarily to the near field. Considering the discussion given here, a symmetric beam is henceforth defined as one that, in its undamaged state, and in the far field, is perfectly or nearly symmetric about midspan. Eq. (3), and the upcoming wavenumber shift expressions derived from Eq. (3), are therefore valid for beams having this generalized symmetry. Note that a beam having this generalized symmetry necessarily has either a deflection node or a deflection anti-node at midspan.

Eq. (3) applies not only to symmetric, lossless beams with classical boundary conditions, but also to symmetric, lossless beams with general, or non-classical, boundary conditions. Eq. (3) is valid, however, only if the non-classical boundaries have a negligible effect on wavenumber shift.[2] But even when the boundary conditions are such that Eq. (3) is valid, Eq. (3) is less accurate near the beam boundaries. The effect of a boundary crack, or a near-boundary crack, varies substantially depending on the boundary. Eq. (3) cannot be accurate near the beam boundaries simply because Eq. (3) gives the same amount of wavenumber shift no matter what the boundary conditions.

Eq. (3) may be rewritten as

$$\sin[\Delta kL - \arctan(\mu)] = \pm \sin[\arctan(\mu)] \cos\left[2k_0\xi_s\left(1 - \frac{\Delta k}{k_0}\right)\right] \tag{4}$$

by using the identities [31, p. 121]

$$u\sin(\theta) \pm v\cos(\theta) = u\sqrt{1 + \left(\frac{v}{u}\right)^2}\sin\left[\theta \pm \arctan\left(\frac{v}{u}\right)\right], \quad u \neq 0$$

and [32, p. 55]

$$\sin[\arctan(u)] = \frac{u}{\sqrt{1+u^2}}.$$

Eq. (4) is a high-frequency characteristic equation for wavenumber shift. The assumptions made so far are higher frequencies, beam symmetry, the crack is in the far field, and the boundaries do not explicitly contribute to wavenumber shift.

A detailed analysis of Eq. (4) reaffirms the well-known result that wavenumber shift is zero when a crack is located where bending stresses are zero. A detailed analysis of Eq. (4) also indicates that, contrary to previous results, the crack locations for which wavenumber shift is a maximum are not, in general, the points in the undamaged beam where bending stress is a maximum. The crack locations of maximum wavenumber shift, however, are close to the points of maximum bending stress in the undamaged beam. Additionally, the crack locations of maximum wavenumber shift vary with crack length. In other words, the maximum wavenumber shift for a crack of length a_1 occurs when the crack is located at point $\xi_{s,1}$. The maximum wavenumber shift for a crack of length a_2, however, occurs when the crack is located at point $\xi_{s,2}$, where point $\xi_{s,2}$ is generally different than point $\xi_{s,1}$. Although the results of the analysis given here indicate that the crack locations of maximum wavenumber shift vary with crack length, the analysis yields the well-known result that if crack length approaches a limiting length of zero, the crack locations of maximum wavenumber shift approach the points of maximum bending stress in the undamaged beam.

[2]In general, a non-classical boundary can contribute to wavenumber shift [13]. The growth of a crack causes a change in a given resonance frequency. If the frequency changes, however, and the boundary impedance varies with frequency, then the boundary impedance also changes. The change in boundary impedance can then cause further change in the resonance frequency. Thus, although the only physical modification in the system is the growth of the crack, both the crack and the boundary can contribute to overall frequency shift or wavenumber shift. Note, however, that although a non-classical boundary *can* affect frequency shift and wavenumber shift, it does not *always* affect frequency shift and wavenumber shift. The effect of a given boundary is determined by the frequency dependence of the boundary impedance (see Ref. [13] for more detail).

Additional approximations are needed to linearize Eq. (4) and obtain an explicit solution for wavenumber shift. First, assume that the change in a resonance wavenumber is much less than the initial resonance wavenumber, or $|\Delta k/k_0| \ll 1$ [13, pp. 33–34, 113, 25, pp. 40–41]. This assumption is a perturbation approximation, and at first glance, appears to limit any subsequent results to the small crack regime. A closer inspection, however, reveals that although the approximation $|\Delta k/k_0| \ll 1$ is better for smaller cracks (and higher frequencies), it is still valid for deeper cracks. The reason that the approximation $|\Delta k/k_0| \ll 1$, or $|\Delta kL/(k_0L)| \ll 1$, is valid for deeper cracks is because dimensionless wavenumber shift ΔkL cannot exceed $\pi/2$ (according to Eqs. (5) and (6)), but the dimensionless absolute wavenumbers k_0L can be much greater than $\pi/2$. As an example, if $\Delta kL = \pi/4$, or half the maximum possible amount of wavenumber shift, and if $k_0L \cong 5\pi/2$ for the second mode of a clamped–clamped beam [28], the crack is deep but the quantity $\Delta kL/(k_0L)$ is only 0.1, a number that can be considered much less than one.

Another approximation needed to linearize Eq. (4) is $\sin[\Delta kL - \arctan(\mu)] \cong \Delta kL - \arctan(\mu)$. This approximation is possible since $0 \leqslant \Delta kL \leqslant \pi/2$, since $0 \leqslant \arctan(\mu) \leqslant \pi/4$, and since both ΔkL and $\arctan(\mu)$ generally increase with increasing crack length. Upcoming wavenumber shift expressions indicate that the quantity $\Delta kL - \arctan(\mu)$ is bounded roughly by $-\pi/4$ and $\pi/4$. The approximation $\sin(\theta) \cong \theta$ is in error by about 10 percent for $\theta \cong \pm \pi/4$, this being a worst-case scenario. The approximation $\sin[\Delta kL - \arctan(\mu)] \cong \Delta kL - \arctan(\mu)$ is better for smaller cracks and for crack locations closer to midspan.

One final approximation needed to linearize Eq. (4) is $\sin[\arctan(\mu)] \cong \arctan(\mu)$. This approximation, possible because $0 \leqslant \arctan(\mu) \leqslant \pi/4$, is in error by about 10 percent near final fracture, this being a worst-case scenario. Incorporating the approximations of this and the previous paragraphs into Eq. (4) and rearranging gives

$$\Delta kL = 2 \arctan\left(\frac{\gamma}{1+\gamma}\right) \cos^2(k_0 \xi_s) \tag{5}$$

for the even-symmetric modes, and

$$\Delta kL = 2 \arctan\left(\frac{\gamma}{1+\gamma}\right) \sin^2(k_0 \xi_s) \tag{6}$$

for the odd-symmetric modes.

Eqs. (5) and (6) indicate that wavenumber shift is approximately proportional to the potential energy in the uncracked beam at the (future) crack location. This result is significant because it indicates that, for a crack in the vibratory far field, wavenumber shift is proportional to potential energy not only for a small crack, a well-known result [8,12,21], but also for a deeper crack.

Eqs. (5) and (6) collapse to explicit expressions given in the literature for a beam with a small, arbitrarily located crack. For example, Eqs. (5) and (6) collapse to expressions given by Morassi [8], Hasan [9], and Liang and Hu [10,11] after assuming $\arctan[\gamma/(1+\gamma)] \cong \gamma$, and after assuming beam deflection is predominantly sinusoidal in space. Additionally, Kasper [13, pp. 57–61] shows the equivalence between Eqs. (5) and (6) and Gudmundson's energy-based expression [12].

Eqs. (5) and (6) are derived using a set of approximations categorized as "high frequency." Eqs. (5) and (6) are also derived using Bernoulli–Euler beam theory and lumped elements. Since Bernoulli–Euler theory and lumped elements are generally applicable only for "low" frequencies, the high-frequency approximations used in the derivation of Eqs. (5) and (6) seem to conflict with the underlying modelling approach. Fortunately, the high-frequency approximations do not render the analysis invalid. Instead, the high-frequency approximations merely introduce a lower frequency limit that would otherwise be absent. As an example, consider the beams used in the experimental portion of this work. For these beams, Eqs. (5) and (6) agreed with the in-plane experimental results for modes two through eight (Eqs. (5) and (6), surprisingly, even agreed with the in-plane experimental results for the fundamental mode, albeit for small defect sizes). Theoretical analysis indicates that Bernoulli–Euler theory was valid for the beams, to within a 10 percent error in wavenumber, up to the 20th mode [13,29, pp. 114–115]. Thus, Bernoulli–Euler theory was valid from the fundamental mode to mode 20, but the high-frequency approximations used in the theoretical analysis limit the results to modes two through 20. So in general, even though Eqs. (5) and (6) are derived using approximations labelled

"high-frequency," Eqs. (5) and (6) are generally valid for a wide range of modes, a range that even includes the lowest beam modes.

Fig. 2 is a plot of normalized wavenumber shift versus crack location ξ_s/L for two values of γ. Normalized wavenumber shift is denoted κ and is defined as $\kappa = \Delta kL/(\pi/2)$. Wavenumber shift ΔkL is normalized by $\pi/2$ because Eqs. (5) and (6) indicate that, for every mode, wavenumber shift ΔkL does not exceed $\pi/2$. The curves in Fig. 2 correspond to the fifth bending mode of a clamped–clamped beam. The solid curves represent wavenumber shift according to the approximate, energy-proportional expression given in Eq. (5), the dashed curves represent wavenumber shift obtained from the high-frequency characteristic equation of Eq. (4), and the dotted curves represent wavenumber shift obtained from the full characteristic equation, Eq. (1). Note that the wavenumber shift curves obtained from the high-frequency characteristic equation (dashed) coincide with the wavenumber shift curves obtained from the exact characteristic equation (dotted) for $|\xi_s/L| \lessapprox 0.33$. The lower set of curves in Fig. 2 corresponds to a small crack ($\gamma = 1/10$), and the upper set of curves corresponds to a deep crack ($\gamma = 1/\sqrt{2}$).

Fig. 2 indicates that the explicit wavenumber shift expressions given in Eqs. (5) and (6) agree well with the exact theory for a wide range of crack locations, and for a wide range of crack depths, including both shallow cracks and deep cracks. Fig. 2 also indicates that, as expected, the explicit wavenumber shift expressions given in Eqs. (5) and (6) are more accurate for smaller cracks and for crack locations closer to midspan. And although not shown in Fig. 2, numerical analysis indicates that the error in the explicit wavenumber shift expressions of Eqs. (5) and (6) generally does not increase with increasing mode number.

The frequency quantity used throughout this paper is wavenumber shift. Wavenumber shift is used rather than frequency shift mainly because the mathematics associated with wavenumber shift are simpler. Explicit expressions for frequency shift, however, may be obtained from the explicit wavenumber shift expressions using the frequency–wavenumber relation

$$\frac{\Delta f}{f_0} = 1 - \left(1 - \frac{\Delta k}{k_0}\right)^2 = 2\frac{\Delta k}{k_0}\left(1 - \frac{1}{2}\frac{\Delta k}{k_0}\right). \tag{7}$$

The frequency–wavenumber relation of Eq. (7) simplifies to

$$\frac{\Delta f}{f_0} = 2\frac{\Delta k}{k_0} \tag{8}$$

if $|\Delta k/(2k_0)| \ll 1$.

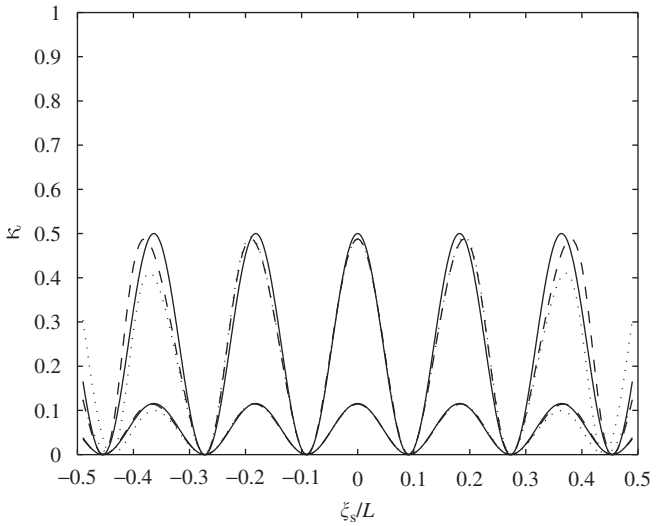

Fig. 2. Theoretical, normalized wavenumber shift κ versus crack location ξ_s/L for the fifth mode of a clamped–clamped beam: Eq. (5) (solid), Eq. (4) (dashed), exact (Eq. (1)) (dotted).

A few authors [6,7,9,23] note that the ratio of frequency (or wavenumber) shift for two different modes depends only on initial frequency and crack location; the ratio does not explicitly depend on crack compliance or on geometric or material parameters. Eqs. (5) through (8) indicate, however, that this frequency shift ratio is independent of crack compliance, geometric parameters, and material parameters only approximately, and only in the small-crack limit. In general, the ratio of frequency or wavenumber shift for two different modes depends on crack compliance and on the beam properties.

4. Relating equivalent compliance to crack length

The wavenumber shift theory given in the previous section relates wavenumber shift to an equivalent crack compliance. To relate wavenumber shift to crack depth rather than to crack compliance, expressions are needed that relate equivalent crack compliance to crack depth. The necessary compliance expressions can be obtained from the fracture mechanics field, using the procedure outlined by each of Dimarogonas and Paipetis [20, pp. 144–148, 160–163], Papaeconomou and Dimarogonas [21], and Tada et al. [33, pp. 487–488]. The procedure involves using Castigliano's theorem, along with the theory of Griffith, Irwin, and Paris.

The equivalent compliance of a transverse, through-the-thickness crack may be written as

$$C_s = \frac{ht}{E}\frac{\partial^2}{\partial M^2}\int_0^{a/h}\int_{-1/2}^{1/2} K_I^2 \,\mathrm{d}(y/t)\,\mathrm{d}(a/h), \tag{9}$$

where y is the coordinate in the thickness direction (see Fig. 1). Eq. (9) incorporates the assumption of mode I loading only. The quantity K_I is therefore the mode I stress-intensity factor. The quantity M in Eq. (9) is a remotely applied bending moment. Eq. (9) represents an energy equivalence, indicating that the energy stored in the equivalent rotational spring is the energy released during crack extension.

The system of interest in this work is a single-edge-notch (SEN) specimen vibrating both in plane and out of plane. An SEN specimen is shown in Fig. 3, along with the definitions of in-plane bending (bending about the strong axis) and out-of-plane bending (bending about the weak axis). For the beams used in the experimental part of this work, the width h of the beams was larger than the thickness t.

For an SEN specimen vibrating in plane [33, pp. 55–56],

$$K_I = \frac{6M}{th^2}\sqrt{\pi a} f_{s,\,\mathrm{in}}\left(\frac{a}{h}\right),$$

where

$$f_{s,\,\mathrm{in}}\left(\frac{a}{h}\right) = \sqrt{\frac{2h}{\pi a}\tan\left(\frac{\pi a}{2h}\right)}\,\frac{0.923 + 0.199[1-\sin((\pi/2)(a/h))]^4}{\cos((\pi/2)(a/h))}.$$

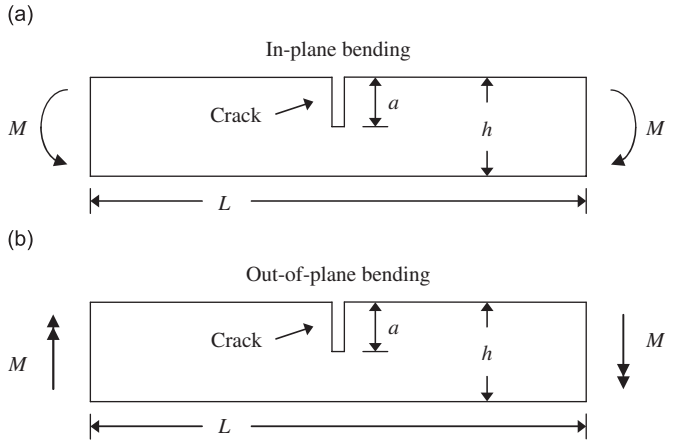

Fig. 3. Definitions of in-plane bending (a) and out-of-plane bending (b) for an SEN specimen.

This stress-intensity factor is accurate to within a half-percent for all a/h. Since the stress-intensity factor is constant along the crack front during in-plane bending, the integral $\int_{-1/2}^{1/2} \mathrm{d}(y/t)$ in Eq. (9) is equal to one. The equivalent crack compliance for an SEN specimen vibrating in plane is therefore given by

$$C_s = \frac{12h}{EI} \int_0^{a/h} \frac{\pi}{2} \frac{a}{h} f_{s,\mathrm{in}}^2 \left(\frac{a}{h}\right) \mathrm{d}(a/h). \tag{10}$$

The equivalent compliance of Eq. (10) is valid only for an open crack.

The equivalent compliance for an SEN specimen bending out of plane is apparently not available in the literature [19]. An appropriate stress-intensity factor is apparently not available either. Fortunately, the equivalent compliance for an SEN specimen bending out of plane can be estimated using the stress-intensity factors for double-edge notch (DEN) and center-cracked (CC) specimens in tension. The DEN stress-intensity factor is appropriate for smaller cracks and the CC stress-intensity factor is appropriate for deeper cracks. The DEN and CC stress-intensity factors can be substituted for the missing SEN stress-intensity factor because a DEN specimen and a CC specimen are each effectively two SEN specimens. In particular, the DEN and CC specimens reflect the minimal in-plane, or lateral, deflection that occurs when an SEN specimen bends out of plane. An SEN specimen, although asymmetric, does not deflect in plane during out-of-plane bending because any in-plane deflection due to out-of-plane, tensile bending stresses is offset by an opposing deflection due to out-of-plane, compressive bending stresses.

The equivalent compliance of an SEN specimen bending out of plane is given approximately by

$$C_s = \frac{4h}{EI} F_{s,\mathrm{out}} \left(\frac{a}{h}\right), \tag{11}$$

where

$$F_{s,\mathrm{out}} \left(\frac{a}{h}\right) = \frac{1}{2} \int_0^{a/h} \tan\left(\frac{\pi}{2} \frac{a}{h}\right) \left[1 + 0.122 \cos^4\left(\frac{\pi}{2} \frac{a}{h}\right)\right]^2 \mathrm{d}(a/h) \tag{12}$$

for a small crack and

$$F_{s,\mathrm{out}} \left(\frac{a}{h}\right) = \frac{1}{2} \int_0^{a/h} \frac{(\pi/2)(a/h)}{\cos((\pi/2)(a/h))} \left[1 - 0.025\left(\frac{a}{h}\right)^2 + 0.06\left(\frac{a}{h}\right)^4\right]^2 \mathrm{d}(a/h) \tag{13}$$

for a deep crack. The DEN stress-intensity factor used in Eq. (12) is accurate to within 0.5% for any a/h and the CC stress-intensity factor used in Eq. (13) is accurate to within 0.1% for any a/h [33, pp. 40–48, 34, pp. 1.4.2-4, 1.4.3-1]. Note that an extra factor of $\frac{1}{2}$ enters into Eqs. (12) and (13) when applying the DEN and CC stress-intensity factors to an SEN specimen. Eqs. (11) through (13) are valid only for open cracks.

5. Experimental apparatus and method

The beams used in the experiments were free–free, SEN beams. Free–free conditions were simulated by suspending a beam with fishing line (Fig. 4). The fishing line, or suspension lines, was looped around the beam at symmetric nodal locations for a single mode of the undamaged beam [27, p. 260]. Each beam was suspended such that gravity acted to bend the beam about its strong axis. This beam orientation was used for both in-plane bending and out-of-plane bending.

Dynamic measurements were made on a free–free beam by impacting the beam at one end and monitoring the resulting free vibration at the other end [35,36]. The free vibration was monitored using microphones located close to the beam. The microphone outputs were amplified, low-pass filtered, and then captured on a two-channel, 16-bit digital signal processing (DSP) board. The DSP board had fourth-order, equal-value, Sallen–Key anti-aliasing filters, each with a cutoff frequency of about 2780 Hz. The sampling rate on the DSP board was 16 kHz.

The DSP board continuously computed 16384-point discrete Fourier transforms (DFT) using the fast Fourier transform algorithm. The DFTs were computed using a Riesz data window [37], 25 percent overlap, and no averaging. Resonance frequencies were obtained from the DFTs using a simple peak-picking

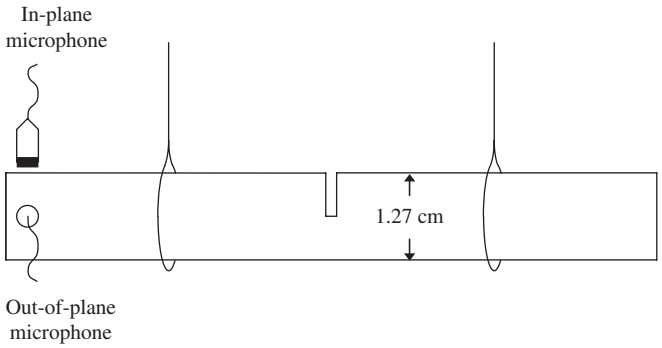

Fig. 4. The free–free beam used in the experiments.

algorithm. Because the beams were lightly damped, the uncertainty in a frequency estimate is approximately $f_s/(2\sqrt{3}N)$ Hz, where f_s is the sampling rate and N is the DFT size [13, pp. 146–148]. With a sampling rate f_s of 16 kHz and a DFT size N of 16 384, the frequency uncertainty is 0.3 Hz.

The normalized wavenumber shift is obtained from frequency using the relation

$$\kappa = \frac{4\sqrt[4]{3}}{\sqrt{\pi}} \frac{L}{\sqrt{h}} \sqrt[4]{\frac{\rho}{E}} (\sqrt{f_0} - \sqrt{f}), \tag{14}$$

where f_0 is the experimental resonance frequency for a given mode of the undamaged beam and f is the experimental resonance frequency of the corresponding mode in the damaged beam. The width h in Eq. (14) is replaced with the thickness t for out-of-plane bending. Eq. (14) is obtained via the dispersion relation for bending (Section 3).

Several preliminary experiments were performed to assess the effect of the suspension lines on wavenumber shift. The results of these experiments indicate that the suspension lines had a negligible effect on wavenumber shift. Results are therefore presented only for one suspension line location, that location being the second-outermost nodes of mode five. The relative locations of the second-outermost nodes of mode five are given by $\xi/L = \pm 0.274$ [38].

The beams used in the experiments were oil-hardening ground flat stock, tool steel AISI-O1. The beams were $1.27 + 0.01$ cm $(0.5 + 0.005$ in) wide by $0.318 + 0.003$ cm $(0.125 + 0.001$ in) thick, according to the manufacturer's specifications. The beams used in the wavenumber shift experiments were milled to a length of 81.359 cm (32 1/32 in). The beams were chosen to be slender so that multiple modes occurred in a relatively small bandwidth.

The longitudinal sound speed $\sqrt{E/\rho}$ of the beams, needed to convert between bending frequency and bending wavenumber (see Eq. (14)), was estimated dynamically using the apparatus shown in Fig. 4. The longitudinal sound speed for the beams is 5181 ± 2 m/s, where the 2 m/s uncertainty represents a standard deviation of the mean with 11 degrees of freedom [39,40, pp. 102–106]. Note that flexural resonance frequencies were used to estimate longitudinal sound speed rather than longitudinal resonance frequencies.

A single-edge slot was introduced at midspan of the free–free beams. Each single-edge slot was assumed to be a suitable substitute for an open crack (see Refs. [13, pp. 81–85, 185, and 19,41]). Slots were cut using a jeweler's saw, the blades for which had a manufacturer-specified width of 0.016 cm (0.0063 in). After cutting, measured slot widths were typically between 0.018 and 0.023 cm at or near the slot tip. The variation in both the width and shape of the slot introduced negligible error into the experiments.

Slot depth was measured optically, on both the fronts and backs of the beams, using a contact reticle and a low-power microscope. A reported slot depth is the average of the individual front and back measurements for a given slot depth. The uncertainty associated with normalized slot depth a/h is 0.002, where the 0.002 uncertainty is a standard deviation of the mean with three degrees of freedom.

Wavenumber shift experiments were performed for four beams. The experimental results were very similar for all four beams. As a result, data is presented for only one beam, that beam being beam 11. Referring to Eq. (14), beam 11 had a width h of 1.2743 ± 0.0007 cm, a thickness t of 0.3188 ± 0.0002 cm, and a length L of 81.359 ± 0.001 cm. Each of the dimensional uncertainties represents a standard deviation of the mean. The width uncertainty of 0.0007 cm and the thickness uncertainty of 0.0002 cm each have seven degrees of freedom, and the length uncertainty of 0.001 cm has three degrees of freedom.

6. In-plane experimental results

Fig. 5 is a comparison between experimental, normalized wavenumber shift and theoretical, normalized wavenumber shift for the in-plane bending modes of beam 11. The solid lines represent experimental data, with pluses denoting the data points. The dotted lines in Fig. 5 represent theoretical wavenumber shift according to the exact, Bernoulli–Euler theory for a cracked, free–free beam [22]. The theoretical curves are generated using experimentally obtained values of width and length. The modes shown in Fig. 5 are, from bottom to top, one, three, five, and seven. These are the lowest four in-plane, even-symmetric modes.[3]

As shown in Fig. 5, the experimental results generally agree well with the exact theory.[4] For modes one and three, the experimental results agree closely with the exact theory for all of the slot depths tested. For mode five, experiment and exact theory agree closely up to a slot depth of about $a/h = 0.75$. Beyond $a/h = 0.75$, the experimental results for mode five differ slightly from the exact theory. For mode seven, experiment and exact theory agree closely up to a slot depth of about $a/h = 0.5$. For deeper slots, however, the experimental results for mode seven deviate significantly from the exact theory. One likely explanation for the discrepancy between experiment and theory for modes five and seven is coupling. Coupling effects, either a result of modal coupling or coupling between beam segments, are reported elsewhere in the literature [15,19,42].

Another comparison of experimental and theoretical wavenumber shifts for beam 11 is given in Fig. 6. The experimental curves in Fig. 6 (solid) are the same as in Fig. 5, but the theoretical curves in Fig. 6 (dashed and dash-dot) are different than those in Fig. 5. The theoretical curves in Fig. 6(a) (dashed) correspond to the explicit, high-frequency theory (Eqs. (5) and (10)), and the theoretical curves in Fig. 6(b) (dash-dot) correspond to the explicit, small-crack theory available in the literature [6,10,11].

The results in Fig. 6 show that, for the fundamental mode, the explicit, high-frequency theory agrees with the experimental wavenumber shift data only for smaller slots. For mode three, the explicit, high-frequency theory agrees with the experimental wavenumber shift data over a wide range of slot depths. For deep slots, however, the high-frequency theory is in slight disagreement with the mode three experimental data. Finally, for modes five and seven, the explicit, high-frequency theory agrees with the experimental wavenumber shift data for the same ranges of slot depth over which the exact theory agrees with the experimental data (Fig. 5).

Still considering the results shown in Fig. 6, the explicit, high-frequency theory is appropriate over a wider range of slot depths than the explicit, small-crack theory for modes three and above. Additionally, for modes three and above, the explicit, high-frequency theory is more accurate than the explicit, small-crack theory for the range of slot depths over which both theories are valid. Finally, from Fig. 6 it can be seen that the small-crack theory generally overestimates wavenumber shift, and can thus underestimate crack depth if the theory is used to estimate crack depth from measured frequencies. Although a comparison with the small-crack theory is not presented for the out-of-plane results (Section 7), the same observations can be made based on the out-of-plane results.

With regard to the fundamental mode, from Fig. 6 it can be seen that the explicit, small-crack theory available in the literature is accurate over a wider range of slot depths than the explicit, high-frequency theory. This result is expected since the explicit, small-crack theory is generally applicable to the lowest beam mode, whereas the explicit, high-frequency theory is generally inapplicable to the lowest beam mode. Note that the

[3]The dimensionless resonance wavenumbers of an uncracked, free–free beam are approximately $kL = m\pi + \pi/2$ at higher frequencies [28], where m is a mode number and $m = 1, 2, 3, \ldots$. Note that odd mode numbers correspond to even-symmetric modes and even mode numbers correspond to odd-symmetric modes.

[4]The error bars associated with both normalized slot depth a/h and normalized wavenumber shift κ are too small to be identified in the plots, and are therefore omitted from all wavenumber shift curves.

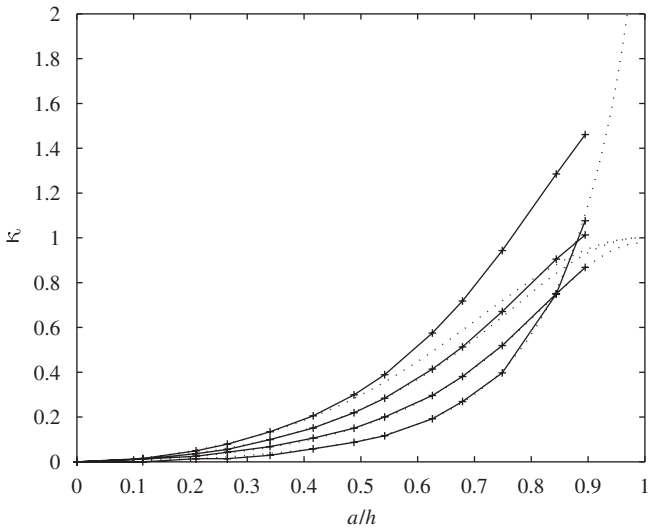

Fig. 5. Normalized wavenumber shift versus normalized slot depth for the first four in-plane, even-symmetric modes: experiment (solid), exact theory from [22] plus Eq. (10) (dotted).

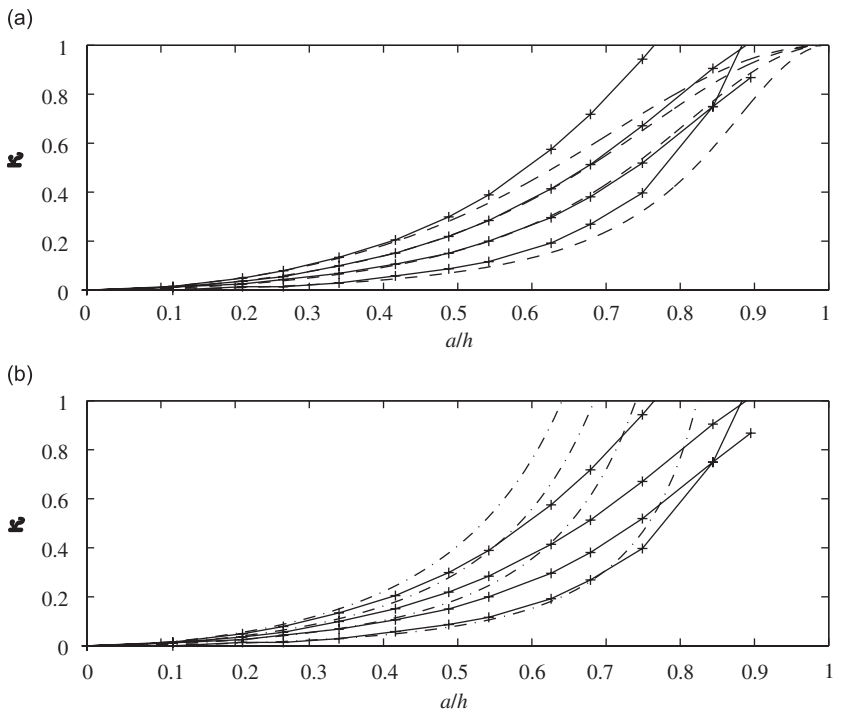

Fig. 6. Normalized wavenumber shift versus normalized slot depth for the first four in-plane, even-symmetric modes: (a) experiment (solid) and Eqs. (5) and (10) (dashed); (b) experiment (solid) and the small-crack theory from Refs. [6,10,11] (dash-dot).

theoretical curves in Figs. 5 and 6 are generated from theory for a cracked beam but the experimental data was obtained from a slotted beam.

Even though the explicit, high-frequency theory is *generally* inapplicable to the fundamental beam mode, from Fig. 6 it can be seen that the high-frequency theory can be appropriate for the fundamental beam mode in specific cases. The applicability of the explicit, high-frequency theory to the fundamental mode depends on

the system characteristics, and therefore varies from system to system. As a result, discussions about the applicability of the explicit, high-frequency theory to the fundamental beam mode are deliberately vague throughout this paper.

The experimental results given so far apply to the in-plane, even-symmetric bending modes. Experiments were also performed, however, for the in-plane, odd-symmetric bending modes. Although not shown here (see Ref. [13] for full results), the experimental results for the in-plane, odd-symmetric modes indicate that, as expected, the odd-symmetric modes shifted minimally over the entire range of slot depths tested. The odd-symmetric modes are those modes for which the slot coincided with the central-most deflection node.

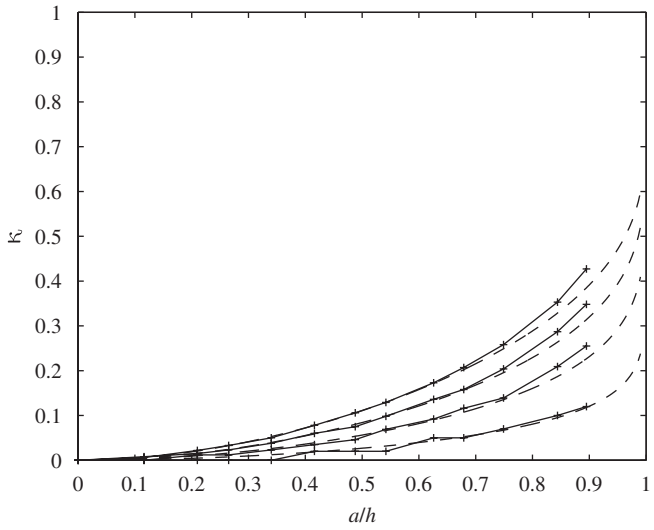

Fig. 7. Normalized wavenumber shift versus normalized slot depth for out-of-plane bending modes three, seven, 11, and 15: experiment (solid), Eqs. (5), (11), and (12) (DEN K_I) (dashed).

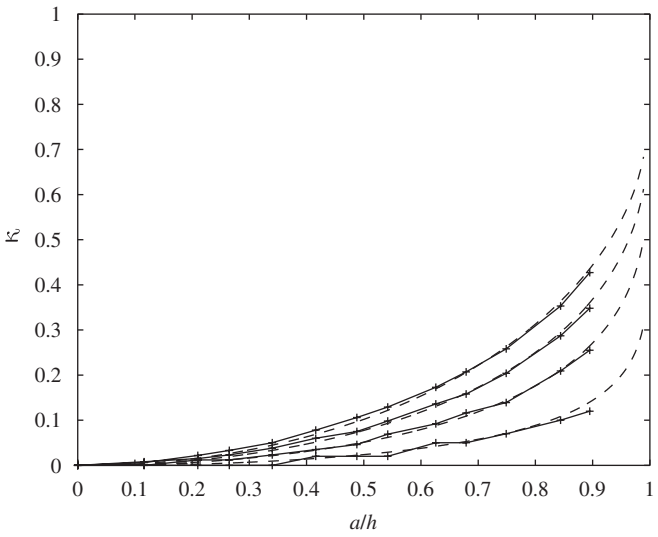

Fig. 8. Normalized wavenumber shift versus normalized slot depth for out-of-plane bending modes three, seven, 11, and 15: experiment (solid), Eqs. (5), (11), and (13) (CC K_I) (dashed).

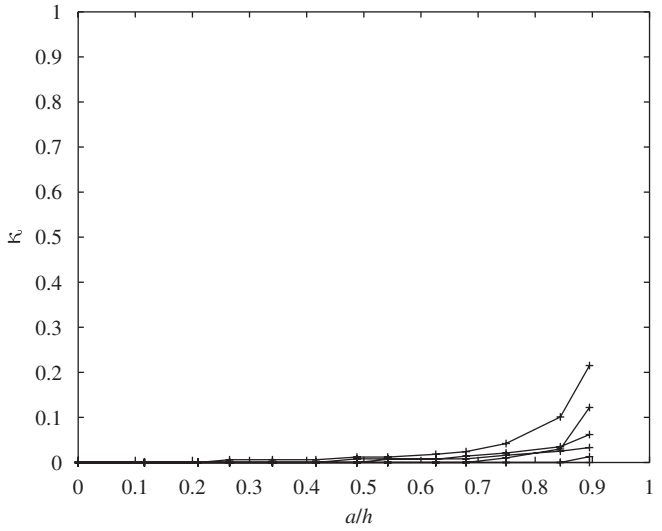

Fig. 9. Normalized wavenumber shift versus normalized slot depth for the out-of-plane, odd-symmetric modes.

7. Out-of-plane experimental results

Figs. 7 and 8 show experimental, normalized wavenumber shift and theoretical, normalized wavenumber shift for four of the out-of-plane bending modes of beam 11. The four modes represented in Figs. 7 and 8 are, from bottom to top, modes three, seven, 11, and 15. Results for modes five, nine, and 13 are not shown, but are very similar to those for modes three, seven, 11, and 15. The explicit, high-frequency theory (Eq. (5)) is used to generate the theoretical curves in both Figs. 7 and 8. Figs. 7 and 8 differ, however, in that the theoretical curves in Fig. 7 are generated using the stress-intensity factor for a DEN specimen in tension (Eqs. (11) and (12)) while the theoretical curves in Fig. 8 are generated using the stress-intensity factor for a CC specimen in tension (Eqs. (11) and (13)).

From Figs. 7 and 8 it can be seen that, overall, the experimental results for out-of-plane bending agree well with the theoretical results. In Fig. 7, experiment and theory agree closely for smaller slots, but not for deeper slots. The lack of agreement for deeper slots is expected, though, since the theoretical curves in Fig. 7 are generated using the stress-intensity factor for a DEN specimen. From Fig. 8 it can be seen that experiment and theory agree for both small and deep slots, but the agreement for smaller slots is not as close as in Fig. 7. Again, this result is expected since the theoretical curves in Fig. 8 are generated using the stress-intensity factor for a CC specimen.

The results given so far in this section apply to the out-of-plane, even-symmetric bending modes. Wavenumber shift results were also obtained, however, for the out-of-plane, odd-symmetric bending modes. These wavenumber shift results are shown in Fig. 9. In increasing order of wavenumber shift at $a/h = 0.895$, the odd-symmetric modes in Fig. 9 are modes four, six, 10, 12, eight, and 14.

The data in Fig. 9 shows that the out-of-plane, odd-symmetric bending modes shifted minimally over a wide range of slot depths. This minimal shift is expected since the odd-symmetric modes had a deflection node that coincided with the slot location. For deep slots, however, some of the odd-symmetric modes shifted more significantly. One possible explanation for the non-negligible wavenumber shift at large slot depths is coupling [15,19,42].

8. Conclusions

Explicit wavenumber shift expressions are derived in Section 3 for a symmetric beam with a crack located in the vibratory far field. These expressions indicate that wavenumber shift is approximately proportional to the potential energy in the uncracked beam at the (future) crack location. This result applies not only to small

cracks, but also to deeper cracks. The explicit, high-frequency wavenumber shift expressions of Section 3 are therefore valid beyond the crack depths where the explicit, small-crack theory available in the literature breaks down. In addition, for higher modes and for cracks in the vibratory far field, the explicit, high-frequency wavenumber shift expressions tend to be more accurate than the explicit, small-crack expressions for the range of crack depths over which both theories are valid.

The wavenumber shift expressions given in Section 3 are initially derived from the characteristic equation for a clamped–clamped beam. These wavenumber expressions can also be derived, however, from characteristic equations given in the literature for beams with other boundary conditions [7,22,23,25]. In addition, the explicit, energy-proportional wavenumber shift expressions given in Eqs. (5) and (6) are equivalent to explicit, small-crack expressions given in the literature (if the crack is assumed to be small, and if beam deflection is assumed to be predominantly sinusoidal in space) [6,8–12]. These equivalences and relationships with previous results not only help validate the explicit, high-frequency theory given here, but also help corroborate and unify the various theories available in the literature.

Although the explicit expressions given here are valid for deeper cracks, the expressions possess a few drawbacks relative to the explicit, small-crack expressions given in the literature. For example, the explicit wavenumber shift expressions given here are limited to symmetric, uniform beams, and are generally inaccurate for the lowest beam mode. In addition, the explicit solutions for wavenumber shift derived here are generally inaccurate for cracks located within a boundary near field.

From the results of Sections 6 and 7 it can be seen that the experimental results, obtained for a beam with a midspan slot, generally agree very well with the theory from Section 3. Theory and experiment agree for a large number of modes, for a wide range of crack or slot depths, and for both in-plane and out-of-plane bending. The experimental results therefore validate the high-frequency theory for the one crack location tested.

The experimental wavenumber shift curves presented in this work represent wavenumber shift for a slotted beam. These experimental wavenumber shift curves agree with theoretical wavenumber shift curves generated from theory for a cracked beam. This agreement between the slotted-beam experimental results and the cracked-beam theory indicates that, from the perspective of wavenumber shift or frequency shift, a beam with a thin slot can be used as a suitable representation of a beam with an open crack.

The results of Sections 6 and 7 indicate that theory and experiment agree not only for the case of an SEN specimen bending in plane, but also for the case of an SEN specimen bending out of plane. Since the out-of-plane equivalent compliance is approximated using stress-intensity factors for DEN and CC specimens (Section 4), the agreement between theory and experiment shown in Section 7 indicates that if an out-of-plane, equivalent compliance for an SEN specimen is unavailable, this equivalent compliance may be approximated using stress-intensity factors for DEN and CC specimens.

Acknowledgements

The authors would like to thank Tom Gabrielson, Cliff Lissenden, Courtney Burroughs, Mark Turner, and Mark Brought for their suggestions throughout this research.

This work was supported through the Applied Research Laboratory Exploratory and Foundational Research program. This work was also supported by the Office of Naval Research under Grant no. N00014-96-1-1147, an Accelerated Capabilities Initiative for Condition-Based Maintenance, and Grant no. N00014-95-1-0461, the Multi-disciplinary University Research Initiative for Integrated Predictive Diagnostics. The content of the information does not necessarily reflect the position or policy of the Government, and no official endorsement should be inferred.

References

[1] G.W. Nickerson, Prognostics: what does it mean in condition-based maintenance? *Proceedings of the 1997 National Conference on Noise Control Engineering* (*NOISE-CON*), Vol. 2, University Park, PA, June 1997, pp. 181–184.

[2] A. Davies (Ed.), *Handbook of Condition Monitoring: Techniques and Methodology*, Chapman & Hall, London, 1998.

[3] J. Wauer, On the dynamics of cracked rotors: a literature survey, *Applied Mechanics Reviews* 43 (1990) 13–17.

[4] A.D. Dimarogonas, Vibration of cracked structures: a state of the art review, *Engineering Fracture Mechanics* 55 (1996) 831–857.
[5] S.W. Doebling, C.R. Farrar, M.B. Prime, A summary review of vibration-based damage identification methods, *The Shock and Vibration Digest* 30 (1998) 91–105.
[6] R.Y. Liang, J. Hu, F. Choy, Theoretical study of crack-induced eigenfrequency changes on beam structures, *Journal of Engineering Mechanics* 118 (1992) 384–396.
[7] Y. Narkis, Identification of crack location in vibrating simply supported beams, *Journal of Sound and Vibration* 172 (1994) 549–558.
[8] A. Morassi, Crack-induced changes in eigenparameters of beam structures, *Journal of Engineering Mechanics* 119 (1993) 1798–1803.
[9] W.M. Hasan, Crack detection from the variation of the eigenfrequencies of a beam on elastic foundation, *Engineering Fracture Mechanics* 52 (1995) 409–421.
[10] J. Hu, R.Y. Liang, An integrated approach to detection of cracks using vibration characteristics, *Journal of the Franklin Institute* 330 (1993) 841–853.
[11] R.Y. Liang, J. Hu, F. Choy, Quantitative NDE technique for assessing damages in beam structures, *Journal of Engineering Mechanics* 118 (1992) 1468–1487.
[12] P. Gudmundson, Eigenfrequency changes of structures due to cracks, notches, or other geometrical changes, *Journal of the Mechanics and Physics of Solids* 30 (1982) 339–353.
[13] D.G. Kasper, The Effect of a Crack or Slot on the Resonance Wavenumbers and Resonance Frequencies of a Vibrating Beam, PhD Thesis, The Pennsylvania State University, 2004.
[14] H.-Y. Chang, H.J. Petroski, On detecting a crack by tapping a beam, *International Journal of Pressure Vessels and Piping* 22 (1986) 41–55.
[15] J. Brandon, Nonlinear vibration of cracked structures: perspectives and horizons, *The Shock and Vibration Digest* 32 (2000) 273–280.
[16] O.S. Salawu, Detection of structural damage through changes in frequency: a review, *Engineering Structures* 19 (1997) 718–723.
[17] R. Gasch, A survey of the dynamic behaviour of a simple rotating shaft with a transverse crack, *Journal of Sound and Vibration* 160 (1993) 313–332.
[18] W. Ostachowicz, M. Krawczuk, On modelling of structural stiffness loss due to damage, *Key Engineering Materials: Damage Assessment of Structures* 204–205 (2001) 185–199.
[19] P. Gudmundson, The dynamic behaviour of slender structures with cross-sectional cracks, *Journal of the Mechanics and Physics of Solids* 31 (1983) 329–345.
[20] A.D. Dimarogonas, S.A. Paipetis, *Analytical Methods in Rotor Dynamics*, Applied Science Publishers, Ltd., London, 1983.
[21] N. Papaeconomou, A.D. Dimarogonas, Vibration of cracked beams, *Computational Mechanics* 5 (1989) 88–94.
[22] M.E. Reznicek, W.T. Springer, Damage assessment of transversely vibrating uniform beams containing a symmetric discontinuity, *Proceedings of the 1985 SEM Spring Conference on Experimental Mechanics*, Las Vegas, NV, June 1985, pp. 404–409.
[23] Y. Narkis, E. Elmalah, Crack identification in a cantilever beam under uncertain end conditions, *International Journal of Mechanical Sciences* 38 (1996) 499–507.
[24] A. Morassi, M. Rollo, Identification of two cracks in a simply supported beam from minimal frequency measurements, *Journal of Vibration and Control* 7 (2001) 729–739.
[25] S.H. Arzoumanian, Crack Detection in Simple and Complex Beam-like Structures using Modal Analysis, MS Thesis, The Pennsylvania State University, 2000.
[26] E. Skudrzyk, *Simple and Complex Vibratory Systems*, The Pennsylvania State University Press, University Park, PA, 1968 (second printing 1981).
[27] J.W. Strutt (Lord Rayleigh), *The Theory of Sound*, Dover Publications, New York, 1877 (re-issued 1945).
[28] R.D. Blevins, *Formulas for Natural Frequency and Mode Shape*, Krieger Publishing Company, Malabar, FL, 1995 (reprinted 2001).
[29] L. Cremer, M. Heckl, *Structure-Borne Sound: Structural Vibrations and Sound Radiation at Audio Frequencies*, second ed., translated by E.E. Ungar, Springer, Berlin, 1987.
[30] F. Fahy, *Sound and Structural Vibration: Radiation, Transmission, and Response*, Academic Press, Inc., San Diego, CA, 1985 (reprinted 1994).
[31] A. Jeffrey, *Handbook of Mathematical Formulas and Integrals*, second ed., Academic Press, San Diego, CA, 2000.
[32] I.S. Gradshteyn, I.M. Ryzhik, *Table of Integrals, Series, and Products*, sixth ed., Academic Press, San Diego, CA, 2000.
[33] H. Tada, P.C. Paris, G.R. Irwin, *The Stress Analysis of Cracks Handbook*, third ed., ASME Press, New York, 2000.
[34] G.C. Sih, *Handbook of Stress-Intensity Factors for Researchers and Engineers: Stress-Intensity Factor Solutions and Formulas for Reference*, Institute of Fracture and Solid Mechanics, Lehigh University, Bethlehem, PA, 1973.
[35] P. Cawley, R. Ray, A comparison of the natural frequency changes produced by cracks and slots, *Journal of Vibration, Acoustics, Stress, and Reliability in Design* 110 (1988) 366–370.
[36] S. Chen, Resonant frequency method for the measurement and uncertainty analysis of acoustic and elastic properties, *Ultrasonics* 38 (2000) 206–211.
[37] F.J. Harris, On the use of windows for harmonic analysis with the discrete Fourier transform, *Proceedings of the IEEE* 66 (1978) 51–84.
[38] American Society for Testing and Materials standard E1875-00, Standard test method for dynamic Young's modulus, shear modulus, and Poisson's ratio by sonic resonance, *Annual Book of ASTM Standards*, Vol. 03.01, 2003, pp. 1099–1106.

[39] American National Standards Institute/NCSL International standard ANSI/NCSL Z540-2-1997, US guide to the expression of uncertainty in measurement, 1997.
[40] J.R. Taylor, *An Introduction to Error Analysis: The Study of Uncertainties in Physical Measurements*, second ed., University Science Books, Sausalito, CA, 1997.
[41] A.J.M.A. Gomes, J.M.M.E. Silva, On the use of modal analysis for crack identification, *Proceedings of the Eighth International Modal Analysis Conference*, Vol. 2, Kissimmee, FL, January/February 1990, pp. 1108–1115.
[42] G. Biscontin, A. Morassi, P. Wendel, Asymptotic separation of the spectrum in notched rods, *Journal of Vibration and Control* 4 (1998) 237–251.